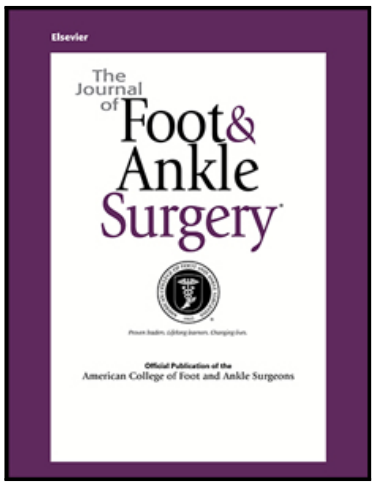

Comparison of Fixation Techniques in Oblique and Biplanar Chevron Medial Malleolar Osteotomies; a Finite Element Analysis

Ali Levent MD Assist. Prof. , Metin Yapti MD ,
H. Kursat Celik PhD Assoc. Prof. , Ozkan Kose MD Assoc. Prof. ,
O. Faruk Kilicaslan MD , Allan E.W. Rennie PhD Prof.

PII: S1067-2516(21)00271-4
DOI: https://doi.org/10.1053/j.jfas.2021.07.017
Reference: YJFAS 53575

To appear in: *The Journal of Foot and Ankle Surgery*

Please cite this article as: Ali Levent MD Assist. Prof. , Metin Yapti MD , H. Kursat Celik PhD Assoc. Prof. , Ozkan Kose MD Assoc. Prof. , O. Faruk Kilicaslan MD , Allan E.W. Rennie PhD Prof. , Comparison of Fixation Techniques in Oblique and Biplanar Chevron Medial Malleolar Osteotomies; a Finite Element Analysis, *The Journal of Foot and Ankle Surgery* (2021), doi: https://doi.org/10.1053/j.jfas.2021.07.017

Comparison of Fixation Techniques in Oblique and Biplanar Chevron Medial Malleolar Osteotomies; a Finite Element Analysis

Ali LEVENT[1], MD, Assist. Prof. dralilevent@hotmail.com ORCID:0000-0002-3666-1084

Metin YAPTI[1], MD metyn99@gmail.com ORCID : 0000-0001-7461-8936

H. Kursat CELİK[2], PhD, Assoc. Prof. hkcelik@akdeniz.edu.tr ORCID:0000-0001-8154-6993

Ozkan KOSE[3], MD, Assoc. Prof. drozkankose@hotmail.com ORCID: 0000-0002-7679-9635

O. Faruk KILICASLAN[3], MD kilicaslanfaruk@hotmail.com ORCID: 0000-0001-6716-4542

Allan E.W. RENNIE[4], PhD, Prof. a.rennie@lancaster.ac.uk ORCID: 0000-0003-4568-316X

1. Department of Orthopedics & Traumatology ,Sanliurfa Mehmet Akif Inan Training and Research Hospital, Health Sciences University, Sanlıurfa, Turkey

2. Department of Agricultural Machinery & Technology Engineering, Akdeniz University, Antalya, Turkey

3. Department of Orthopedics and Traumatology, Antalya Training & Research Hospital, Antalya, Turkey

4. Department of Engineering, Lancaster University, Lancaster, United Kingdom

Corresponding author: Dr. Ozkan KOSE

Address : Antalya Egitim ve Arastırma Hastanesi, Soğuksu mah. Kazım Karabekir cd. Muratpaşa, 07100, Antalya, Turkey

E-mail : drozkankose@hotmail.com

GSM : + 90 532 642 26 12

Comparison of Fixation Techniques in Oblique and Biplanar Chevron Medial Malleolar Osteotomies; a Finite Element Analysis

Abstract

This study aimed to evaluate different fixation techniques and implants in oblique and biplanar chevron medial malleolar osteotomies using finite element analysis. Both oblique and biplanar chevron osteotomy models were created, and each osteotomy was fixed with two different screws (3.5 mm cortical screw and 4.0 mm malleolar screw) in two different configurations; (1) two perpendicular screws, and (2) an additional third transverse screw. Nine simulation scenarios were set up, including eight osteotomy fixations and the intact ankle. A bodyweight of 810.44 N vertical loading was applied to simulate a single leg stand on a fixed ankle. Sliding, separation, frictional stress, contact pressures between the fragments were analyzed. Maximum sliding (58.347µm) was seen in oblique osteotomy fixed with two malleolar screws, and the minimum sliding (17.272 µm) was seen in chevron osteotomy fixed with three cortical screws. The maximum separation was seen in chevron osteotomy fixed with two malleolar screws, and the minimum separation was seen in oblique osteotomy fixed with three cortical screws. Maximum contact pressure and the frictional stress at the osteotomy plane were obtained in chevron osteotomy fixed with three cortical screws. The closest value to normal tibiotalar contact pressures was obtained in chevron osteotomy fixed with three cortical screws. This study revealed that cortical screws provided better stability compared to malleolar screws in each tested osteotomy and fixation configuration. The insertion of the third transverse screw decreased both sliding and separation. Biplanar chevron osteotomy fixed with three cortical screws was the most stable model.

Keywords: finite element analysis, medial malleolar osteotomy, screw fixation, biplanar chevron osteotomy, oblique osteotomy, biomechanics

Level of evidence: Level 5, Computer model study

Introduction

Medial malleolar osteotomy (MMO) is a well-known surgical approach that may be required for the treatment of large osteochondral lesions of the talus (OLT), mainly when osteochondral autograft transplantation (OAT) is selected (1). The OAT procedure requires perpendicular access to the talar dome to prevent angled insertion of the osteochondral plugs. Perpendicular insertion of osteochondral plugs is crucial to restore the articular congruence and to simulate the native joint contact pressures (2, 3). Various configuration of MMO has been described so far, but the most convenient osteotomy types for OAT procedure is the oblique and the bi-planar chevron type osteotomies (4-12). When performed with an appropriate technique, these two osteotomies provide an adequate surgical field to reach the talus dome (5,9,13).

However, many authors reported that the plane of the osteotomy should be created up to 60° relative to the horizontal plane for perpendicular access to the talar dome. Although an MMO adequately increases the surgical field, the osteotomy itself may be the source of some complications and bring about some challenges such as non-union, malunion, delayed weight bearing, and hardware-related problems (14, 15). Among these problems, malunion is particularly important because earlier biomechanical studies have shown that even 1 mm of displacement or step-off on the medial malleolus significantly increases the contact pressure of the ankle joint that may eventually lead to osteoarthritis (16). Therefore, anatomic reduction, stable fixation, and maintenance of the fixation until the union of the osteotomy are crucial to prevent complications. Besides, the fixation should be stable enough to allow early rehabilitation and weight bearing to preserve ankle movements and muscle mass.

Currently, two parallel screws inserted perpendicular to the osteotomy plane is usually advocated. Nevertheless, some authors suggested that this fixation is insufficient, and an additional parallel screw should be placed in order to prevent vertical migration of the oblique (around 60°) osteotomy (17). Moreover, some other authors argued that MMO should be fixed with a buttress plate, claiming high malunion and non-union rates (14). Current information in the literature on how to fix both oblique and biplanar chevron MMOs is contradictory and insufficient. Unfortunately, there is no biomechanical study on this subject. The biplanar chevron osteotomy is a pyramid-shaped osteotomy with two planes, which has been accepted to have inherent stability (5, 18). In contrast, the oblique osteotomy is a single-plane osteotomy and theoretically more prone to vertical sliding (14, 19). We hypothesized that each MMO type requires different fixation techniques and implants due to their different three-dimensional shape. The current study aimed to evaluate different fixation techniques and implants in oblique and biplanar chevron MMOs utilizing finite element analysis (FEA).

Materials and methods

Study design

This study is a finite element method-based analysis study that is performed under consideration of linear static loading conditions and homogenous isotropic linear elastic material model assumptions. Furthermore, nonlinear contact behavior between related components was defined. Both oblique and biplanar chevron MMOs were created, and each osteotomy was fixed with two different screws in two different configurations. A total of nine simulation scenarios were set up, including eight osteotomy fixations and the intact ankle joint as a control.

Modeling of the ankle joint and osteotomies

An intact ankle joint was modeled based on computerized tomography (CT) data of a patient in order to create a realistic digital model. The patient was a male subject who was 84 cm in height and 98 kg in weight. The CT examination was performed due to a suspicious

fracture following an ankle sprain in the ED. He was otherwise healthy without a previous history of ankle trauma and congenital or acquired deformity. No osseous lesions were detected on the CT, which was reviewed by one experienced radiologist and one orthopedic surgeon. CT examination was performed using the CT device (Siemens go. Up, Siemens, Munich, Germany) installed in the authors' institution. The scan parameters were as follows:130 KV and 42 mA a slicing distance of 0.7 mm from 80 mm above the ankle joint down to the heel in the supine position, a total of 334 axial slices. Written informed consent was taken from the patient to use the imaging files anonymously. 3D Slicer v.4.10.2 (3D Slicer, BWH, Boston, MA, USA), Meshmixer v.3.5 (Autodesk, San Rafael, CA, USA), SolidWorks 2020 (Dassault Systemes SolidWorks Corp, Waltham, USA), and ANSYS Workbench 17.0 (ANSYS, Ltd., Canonsburg, PA, USA) were employed in order to model and simulate the FEA scenarios, respectively.

Both the oblique and biplanar chevron osteotomies were created at a 60° angle with the horizontal plane on the coronal plane following the previously described techniques (17-19). The biplanar chevron osteotomy had two equal osteotomy planes separated from each other with 142° on the axial plane. A 4.0 mm partially threaded malleolar screw and a 3.5 mm full threaded cortical screw made of Ti–6Al–4V (Ti G5) alloy were used for the fixation. Each osteotomy was fixed with two different screw configurations, either with two or three screws, as shown in **Figure 1**. No gap existed between the osteotomized medial malleolar fragment and the tibia.

Boundary conditions and material properties

The ankle joint model was loaded to simulate a single leg stance weight-bearing in a neutral position. The patient's weight (98 kg) was the reference loading magnitude at this stance, and the main load was undertaken by fibular and tibial columns. Wang et al. reported that the human tibia and fibula share the axial loading magnitude with a ratio of 84.3 % and 15.7 %, respectively (20). The loading magnitude carried by the tibial column was calculated as 810.44 N (98 kg x 9.81 m s^{-2} x 0.843) (embedded gravity effect), and this was assigned in

the simulations. The contact definitions between components were included as frictional contact (nonlinear contact) between screw-bone surfaces and the tibiotalar articular cartilage surfaces. Furthermore, bonded contact definitions were defined between cortical and trabecular bone and subcortical bone and the articular cartilage. A screw preload of 2.5 N was also considered in order to obtain realistic simulation results of the fixed fragments and screw performance **(Fig.2).** The coefficients of friction are presented in **Table 1** (21-25).

The material properties defined in the FEA were collected from previous literature. The material properties for cortical, trabecular, and articular cartilage were separately assigned under consideration of isotropic homogenous linear elastic material model assumptions (**Table. 2**) (26-34).

Mesh structure and quality verification

It has been shown that the mesh structure of the model has a direct effect on the results of FEA, and minimum requirements for model selection, proper parameter identification, and verification has been described to obtain an accurate output (35). Thus, both mesh density (sensitivity) analysis and skewness metric (mesh quality) checks were employed in order to verify the FE model for the predefined FEA scenarios. The results of the mesh sensitivity study advised the minimum element size of 1 mm for tibial cortical and trabecular bone. Additionally, the average skewness values of 0.217 and 0.235 were obtained for intact tibia and fixation scenarios, respectively. These skewness values correspond to the minimum element size of 1 mm indicated an excellent mesh quality for the FE Models. With this verification, an identical curvature meshing strategy was utilized for all simulation scenarios. Dell Precision M4800 Series (Intel Core™ i7-4910MQ CPU @ 2.90GHz, NVIDIA Quadro K2100M-2GB, and Physical Memory: 32 GB) mobile workstation was employed as the solving platform.

Calculation of sliding and separation

The maximum displacement of the osteotomized medial malleolar fragment in the y-axis was calculated and recorded as the sliding distance. The maximum perpendicular displacement between the proximal tibia and osteotomized medial malleolar fragment in the x-axis was calculated and recorded as the separation (gap) distance (**Fig. 3**). In addition to visual outputs, numerical values of the equivalent (Von-Mises) stress and total tibiotalar structure deformation distributions on the components, tibiotalar articular cartilage contact pressure, frictional stress, and contact pressure between osteotomy fragments were extracted from the simulation results.

Results

Maximum sliding (58.347 microns) was seen in oblique osteotomy fixed with two malleolar screws (OO-2M), and the minimum sliding (17.272 microns) was seen in chevron osteotomy fixed with three cortical screws (BCO-3C). The maximum separation was seen in chevron osteotomy fixed with two malleolar screws (BCO-2M), and the minimum separation was seen in oblique osteotomy fixed with three cortical screws (BCO-3C). Maximum contact pressure and the frictional stress at the osteotomy plane were obtained in chevron osteotomy fixed with three cortical screws (BCO-3C). The closest value to normal tibiotalar articular contact pressures was obtained in chevron osteotomy fixed with three cortical screws (BCO-3C). The summary of the results is presented in **Figure 4.**

Under defined boundary conditions, any permanent deformation or damage was not detected on any of the analyzed components; cortical bone, trabecular bone, cartilage, and the screws. Maximum equivalent (Von-Mises) stress values on each component were far less than their yield stress points reported in previous studies (26, 29, 33, 36-41). Visual simulation outputs of each scenario are presented in **Figure 5.**

Discussion

In this study, the most commonly used MMO types and fixation techniques were analyzed by means of FEA. The results of this study showed that cortical screws provided

more stable fixation compared to malleolar screws in each tested configuration. The AO foundation traditionally recommends two parallel 40 mm length 4.0 mm diameter partially threaded cancellous screws (malleolar screws) for the fixation of the transverse and oblique medial malleolar fractures (42). Because an MMO is a controlled medial malleolar fracture, the same principles can be used for the choice of fixation technique. In contrast to current recommendations, fixation with full thread cortical screws resulted in less sliding and gap formation in this study. Thus, the use of full thread cortical screws instead of malleolar screws might be advocated during the fixation of MMOs. There are two previous studies that support our findings in the current literature. Parker et al. compared 4.0 mm malleolar screws and 4.0 mm cortical screws with different lengths in a cadaver model of medial malleolar fracture. The authors found that 30 mm 4.0 mm cortical screws were stiffer than malleolar screws (43). A possible explanation for this result lies in the length of the threads and the anatomy of the distal tibia. The purchase of the threads throughout its socket is greater in cortical screws. Secondly, the proximal trabecular bone loses its density towards the proximal tibia and becomes a hollow intramedullary space. Thus, the purchase of shorter screws would be higher compared to longer screws. Pollard et al. compared the pullout strength of two bicortical 3.5mm cortical screws and 4.0mm partially threaded cancellous screws for the fixation of medial malleolar fractures in a cadaver model (44). The average pullout strength of cortical screws was almost three times greater (116.2 N vs. 327.6 N) in cortical screws than the malleolar screws. Similarly, in the current study, equivalent (Von-mises) stresses were accumulated around the proximal shaft of the screws, but it was almost uniformly distributed throughout the cortical screws. Despite the fact that the diameter of cortical screws is less than malleolar screws (3.5mm vs. 4.0mm), they provided better fixation stability.

Secondly, three screw fixations resulted in less sliding and gap formation in both osteotomy types compared to two screw configurations. An additional third transverse screw was first recommended by Kennedy et al. to prevent the superior migration of the osteotomy

fragment (17). However, this proposal was based on their clinical experience but not based on biomechanical testing or experiment. The problems with two screws fixation have also been reported in previous clinical studies. Bull et al. reported that loss of reduction and step-off at the articular surface was seen in 30% of their patients who underwent biplanar chevron MMO (14). Similarly, Gaulrapp et al. reported around 50% malunion and consequent ankle joint osteoarthritis in their clinical study with oblique MMO (45). Based on our findings and previous clinical studies, a third transverse screw may be recommended for both osteotomy type.

Biplanar chevron medial malleolar osteotomy has been claimed to be inherently stable and has been popularized by several surgeons, although there is no biomechanical study (5,9,18,46). In our study, it has been shown that biplanar chevron MMO apparently has less sliding than oblique MMO. However, the gap formation was less in oblique osteotomy with the same fixation technique. Looking at the stress analysis, it is seen that the stress is concentrated at the apex of the pyramid-shaped chevron osteotomy and the frictional forces across the osteotomy plane were higher compared to oblique osteotomy. This mechanical behavior of the chevron osteotomy prevented sliding; however, the apex of the osteotomy acted as a fulcrum point and resulted in varus deformation and gap formation. In the oblique osteotomy, on the other hand, since the stress is distributed along the surface of the single plane osteotomy, sliding occurred rather than the gap formation. It can be claimed that the biplanar chevron osteotomy is more resistant to sliding, but it also appears to be disadvantageous in terms of gap formation. However, this disadvantage can be compensated by the insertion of the third transverse screw.

This study suffers from a number of limitations, notably related to the methods used in FEA. Although FEA is a useful complementary tool to understand the mechanical behavior of biological materials, it is prone to several errors during each step of the analysis (47). The ankle joint is a complex anatomical structure composed of several bones, ligaments, tendons, muscles, and surrounding soft tissues. Unfortunately, simplified assumptions in

describing this complex anatomy under several boundary conditions were applied. Secondly, these approximations may result in numerical solution errors, which should be carefully interpreted by considering the real-life conditions. Although the results of this study were not verified with a cadaveric study, it is still valuable and provides important information about the behavior of different fixation techniques used for MMO.

In conclusion, MMO is a secondary source of complications and must be managed correctly in all steps, from the creation of osteotomy to the fixation. In the light of the results obtained from this study, it was clearly observed that cortical screws are superior to malleolar screws, and the third transverse screw reduces sliding and gap formation. A biplanar chevron MMO fixed with three cortical screws was found to be the most advantageous osteotomy and fixation technique among tested models. If the surgeon is experienced in performing the oblique osteotomy, again, three cortical screw fixation is advocated. This study can be considered as the first study that investigates the fixation techniques in MMOs. Additionally, this study provides a well-described FEA study design and a useful 'how-to-do' strategy for informing further research on complicated stress and deformation analysis of MMOs through advanced engineering simulation techniques.

References

1. Navid DO, Myerson MS. Approach alternatives for treatment of osteochondral lesions of the talus. Foot Ankle Clin. 2002;7(3):635-49.

2. Koh JL, Kowalski A, Lautenschlager E. The effect of angled osteochondral grafting on contact pressure: a biomechanical study. Am J Sports Med. 2006;34(1):116-9.

3. Muir D, Saltzman CL, Tochigi Y, Amendola N. Talar dome access for osteochondral lesions. Am J Sports Med. 2006;34(9):1457-63.

4. Alexander IJ, Watson JT. Step-cut osteotomy of the medial malleolus for exposure of the medial ankle joint space. Foot Ankle. 1991;11(4):242-3.

5. Cohen BE, Anderson RB. Chevron-type transmalleolar osteotomy: an approach to medial talar dome lesions. Techniques in Foot & Ankle Surgery. 2002;1(2):158-162.

6. Lee KB, Yang HK, Moon ES, Song EK. Modified step-cut medial malleolar osteotomy for osteochondral grafting of the talus. Foot Ankle Int. 2008;29(11):1107-10.

7. Mendicino RW, Lee MS, Grossman JP, Shromoff PJ. Oblique medial malleolar osteotomy for the management of talar dome lesions. J Foot Ankle Surg. 1998;37(6):516-23.

8. Oznur A. Medial malleolar window approach for osteochondral lesions of the talus. Foot Ankle Int. 2001;22(10):841-2.

9. O'Farrell TA, Costello BG. Osteochondritis dissecans of the talus. The late results of surgical treatment. J Bone Joint Surg Br. 1982;64(4):494-7.

10. Ray RB, Coughlin EJ Jr. Osteochondritis dissecans of the talus. J Bone Joint Surg Am. 1947;29(3):697-706.

11. Spatt JF, Frank NG, Fox IM. Transchondral fractures of the dome of the talus. J Foot Surg. 1986;25(1):68-72.

12. Wallen EA, Fallat LM. Crescentic transmalleolar osteotomy for optimal exposure of the medial talar dome. J Foot Surg. 1989;28(5):389-94.

13. Sripanich Y, Dekeyser G, Steadman J, Rungprai C, Haller J, Saltzman CL, Barg A. Limitations of accessibility of the talar dome with different open surgical approaches. Knee Surg Sports Traumatol Arthrosc. 2020 Jun 29. https://doi: 10.1007/s00167-020-06113-2. [Epub ahead of print].

14. Bull PE, Berlet GC, Canini C, Hyer CF. Rate of Malunion Following Bi-plane Chevron Medial Malleolar Osteotomy. Foot Ankle Int. 2016;37(6):620-6.

15. Leumann A, Horisberger M, Buettner O, Mueller-Gerbl M, Valderrabano V. Medial malleolar osteotomy for the treatment of talar osteochondral lesions: anatomical and morbidity considerations. Knee Surg Sports Traumatol Arthrosc. 2016;24(7):2133-9.

16. Lareau CR, Bariteau JT, Paller DJ, Koruprolu SC, DiGiovanni CW. Contribution of the medial malleolus to tibiotalar joint contact characteristics. Foot Ankle Spec. 2015 ;8(1):23-8.

17. Kennedy JG, Murawski CD. The Treatment of Osteochondral Lesions of the Talus with Autologous Osteochondral Transplantation and Bone Marrow Aspirate Concentrate: Surgical Technique. Cartilage. 2011;2(4):327-36.

18. Lamb J, Murawski CD, Deyer TW, Kennedy JG. Chevron-type medial malleolar osteotomy: a functional, radiographic and quantitative T2-mapping MRI analysis. Knee Surg Sports Traumatol Arthrosc. 2013;21(6):1283-8.

19. van Bergen CJ, Tuijthof GJ, Sierevelt IN, van Dijk CN. Direction of the oblique medial malleolar osteotomy for exposure of the talus. Arch Orthop Trauma Surg. 2011;131(7):893-901.

20. Wang Q, Whittle M, Cunningham J, Kenwright J. Fibula and its ligaments in load transmission and ankle joint stability. Clin Orthop Relat Res. 1996;(330):261-70.

21. Hayden LR, Escaro S, Wilhite DR, Hanson RR, Jackson RL. A Comparison of Friction Measurements of Intact Articular Cartilage in Contact with Cartilage, Glass, and Metal. J Biomimetics, Biomater Biomed Eng. 2019;41:23–35.

22. Gao X, Fraulob M, Haïat G. Biomechanical behaviours of the bone-implant interface: a review. J R Soc Interface. 2019;16(156):20190259.

23. Hayes WC, Perren SM. Plate-bone friction in the compression fixation of fractures. Clin Orthop Relat Res. 1972;89:236-40.

24. Eberle S, Gerber C, von Oldenburg G, Högel F, Augat P. A biomechanical evaluation of orthopaedic implants for hip fractures by finite element analysis and in-vitro tests. Proc Inst Mech Eng H. 2010;224(10):1141-52.

25. Marvan J, Horak Z, Vilimek M, Horny L, Kachlik D, Baca V. Fixation of distal fibular fractures: A biomechanical study of plate fixation techniques. Acta Bioeng Biomech. 2017;19(1):33-39.

26. Dong XN, Acuna RL, Luo Q, Wang X. Orientation dependence of progressive post-yield behavior of human cortical bone in compression. J Biomech 2012;45:2829–34.

27. Wang X, Nyman JS, Dong X, Leng H, Reyes M. Fundamental Biomechanics in Bone Tissue Engineering. Synth Lect Tissue Eng. 2010;2(1):1-225.

28. Kim SH, Chang SH, Jung HJ. The finite element analysis of a fractured tibia applied by composite bone plates considering contact conditions and time-varying properties of curing tissues. Compos Struct. 2010;92(9):2109-2118.

29. Klekiel T, Bedzinski R. Finite element analysis of large deformation of articular cartilage in upper ankle joint of occupant in military vehicles during explosion. Archives of Metallurgy and Materials. 2015;60(3):2115-2121. https://doi.org/10.1515/amm-2015-0356

30. Alonso-Rasgado T, Jimenez-Cruz D, Karski M. 3-D computer modelling of malunited posterior malleolar fractures: effect of fragment size and offset on ankle stability, contact pressure and pattern. J Foot Ankle Res. 2017;10:13.

31. Anderson DD, Goldsworthy JK, Li W, James Rudert M, Tochigi Y, Brown TD. Physical validation of a patient specific contact finite element model of the ankle. J Biomech. 2007;40(8):1662-9.

32. Zhu ZJ, Zhu Y, Liu JF, Wang YP, Chen G, Xu XY. Posterolateral ankle ligament injuries affect ankle stability: a finite element study. BMC Musculoskelet Disord. 2016;17:96.

33. Oldani C, Dominguez A. Titanium as a biomaterial for implants. In: S Fokter, ed. Recent Advances in Arthroplasty, InTech, 2012:149–162.

34. Novitskaya E, Zin C, Chang N, Cory E, Chen P, D'Lima D, Sah RL, McKittrick J. Creep of trabecular bone from the human proximal tibia. Mater Sci Eng C Mater Biol Appl. 2014;40:219-27.

35. Viceconti M, Olsen S, Nolte LP, Burton K. Extracting clinically relevant data from finite element simulations. Clin Biomech 2005;20:451–4.

36. Ding M, Dalstra M, Danielsen CC, Kabel J, Hvid I, Linde F. Age variations in the properties of human tibial trabecular bone. J Bone Joint Surg Br. 1997;79(6):995-1002.

37. Jensen NC, Hvid I, Krøner K. Strength pattern of cancellous bone at the ankle joint. Eng Med. 1988 Apr;17(2):71-6.

38. Klekiel T, Wodzisławski J, BeRdzinski R. Modelling of damping properties of articular cartilage during impact load. Eng Trans. 2017;65:133–145

39. Morgan EF, Unnikrisnan GU, Hussein AI. Bone Mechanical Properties in Healthy and Diseased States. Annu Rev Biomed Eng. 2018;20:119–43.

40. Park S, Lee S, Yoon J, Chae SW. Finite element analysis of knee and ankle joint during gait based on motion analysis. Med Eng Phys. 2019;63:33–41.

41. Sierpowska J, Hakulinen MA, Töyräs J, Day JS, Weinans H, Jurvelin JS, Lappalainen R. Prediction of mechanical properties of human trabecular bone by electrical measurements. Physiol Meas. 2005;26(2):S119-31.

42. ORIF for Infrasyndesmotic, medial fracture with lateral fracture/avulsion n.d. https://surgeryreference.aofoundation.org/orthopedic-trauma/adult-trauma/malleoli/infrasyndesmotic-medial-fracture-with-lateral-fracture-avulsion/orif. Accessed September 15, 2020.

43. Parker L, Garlick N, McCarthy I, Grechenig S, Grechenig W, Smitham P. Screw fixation of medial malleolar fractures: a cadaveric biomechanical study challenging the current AO philosophy. Bone Joint J. 2013;95-B(12):1662-6.

44. Pollard JD, Deyhim A, Rigby RB, Dau N, King C, Fallat LM, Bir C. Comparison of pullout strength between 3.5-mm fully threaded, bicortical screws and 4.0-mm partially threaded, cancellous screws in the fixation of medial malleolar fractures. J Foot Ankle Surg. 2010;49(3):248-52.

45. Gaulrapp H, Hagena FW, Wasmer G. Postoperative rating of osteochondritis dissecans of the talus with special respect to medial malleolar osteotomy. Z Orthop Ihre Grenzgeb. 1996;134:346–53.

46. Granata JD, DeCarbo WT, Hyer CF, Granata AM, Berlet GC, Stansbury E. Exposure of the Medial Talar Dome: Bi-Plane Chevron Medial Malleolus Osteotomy. Foot Ankle Spec. 2013;6:12-14.

47. Cheung JTM, Zhang M. A 3-dimensional finite element model of the human foot and ankle for insole design. Arch Phys Med Rehabil. 2005;86:353–8.

Tables

Table 1. Friction coefficients and screw fixation preload assigned in the FEA set up. References are provided as uppercase numbers.

Table 2. Material properties assigned in the FEA set up in accordance with the homogenous isotropic linear elastic material model. References are provided as uppercase numbers.

Figure Legends

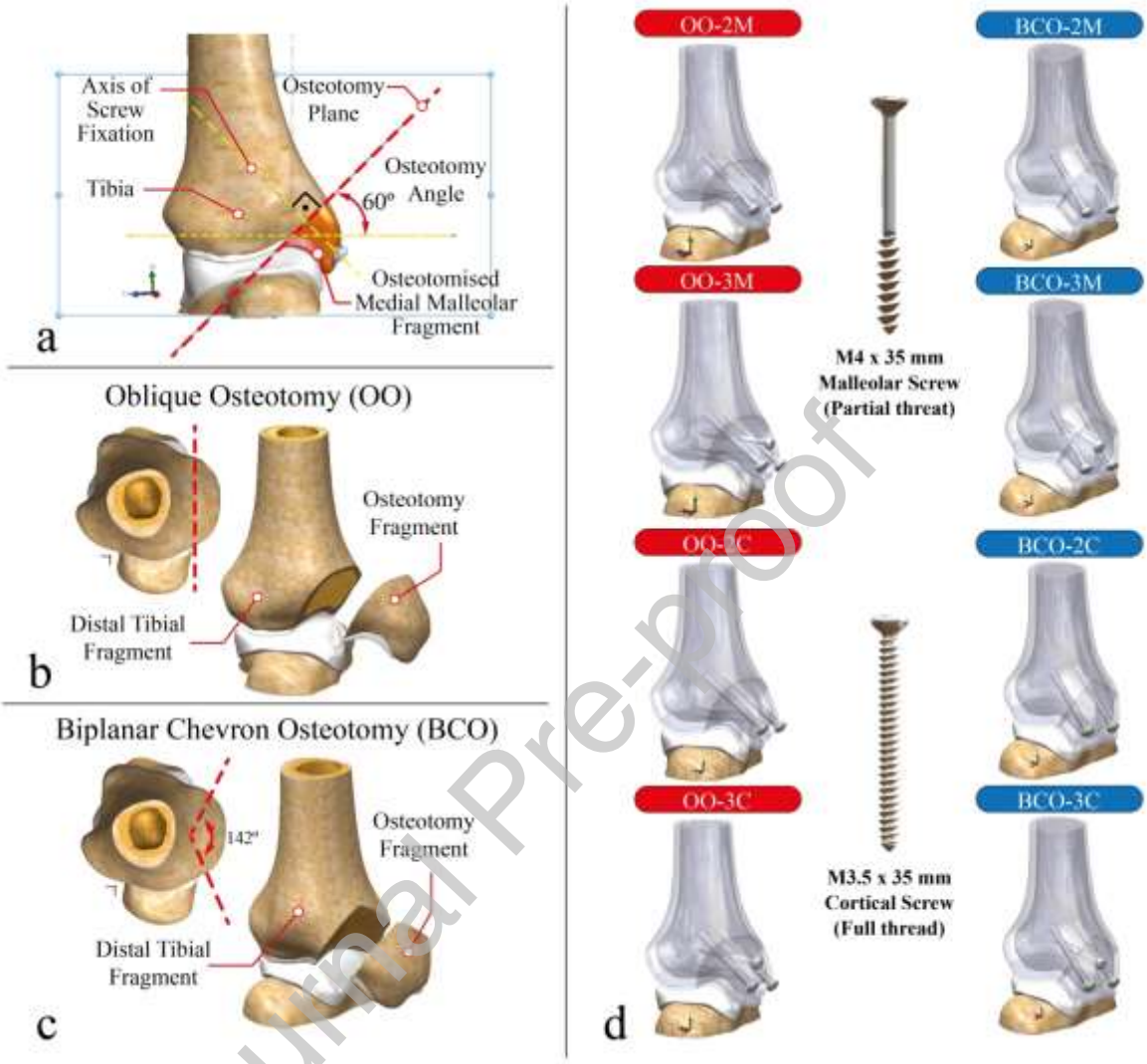

Figure 1. (a) The osteotomy was created at a 60° angle with the horizontal plane, and the screws were inserted perpendicular to the osteotomy plane. (b) Model of the oblique osteotomy. (c) Model of the biplanar chevron osteotomy. (c) Solid models showing the configuration of the screw fixation and the type of screws.

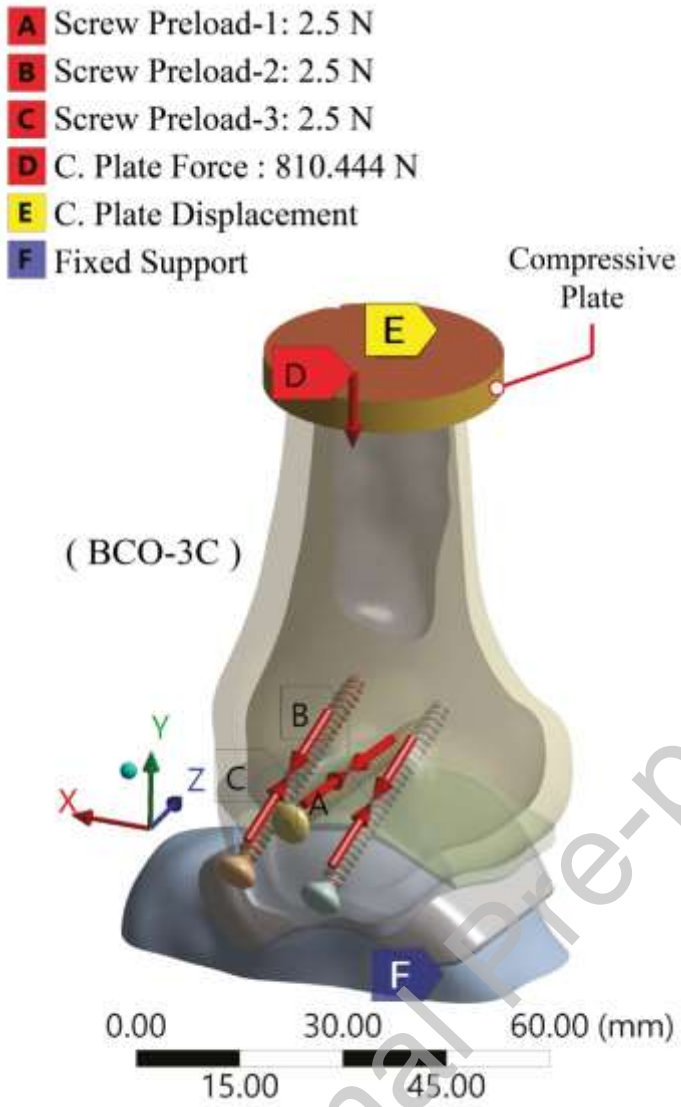

Figure 2. The boundary conditions that are assigned in the simulation scenarios. Biplanar chevron osteotomy fixed with three cortical screws (BCO-3C) is illustrated as a sample.

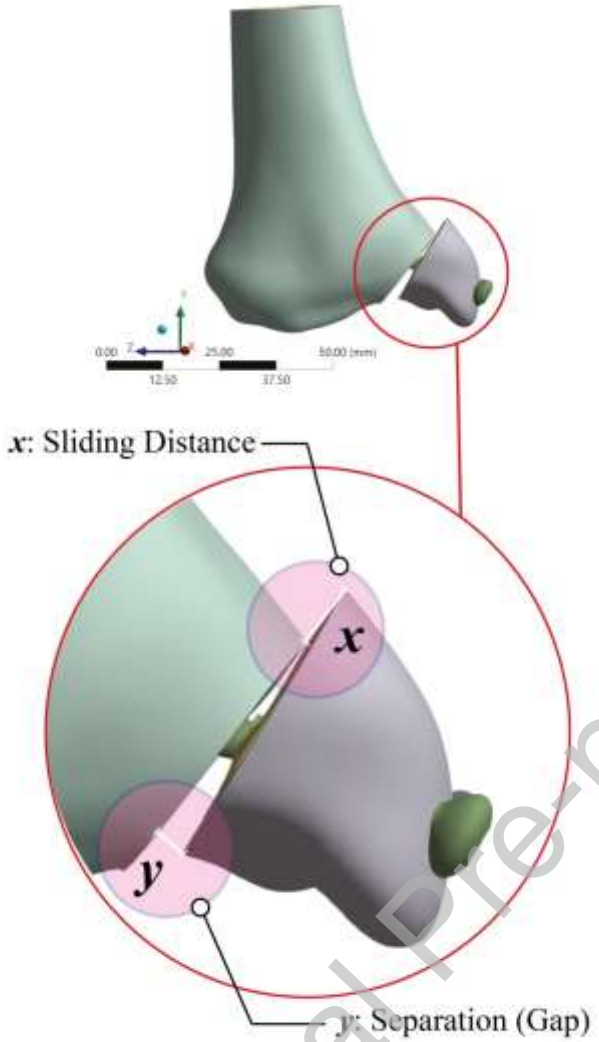

Figure 3. Illustration showing the measurement of sliding and the gap formation between fragments.

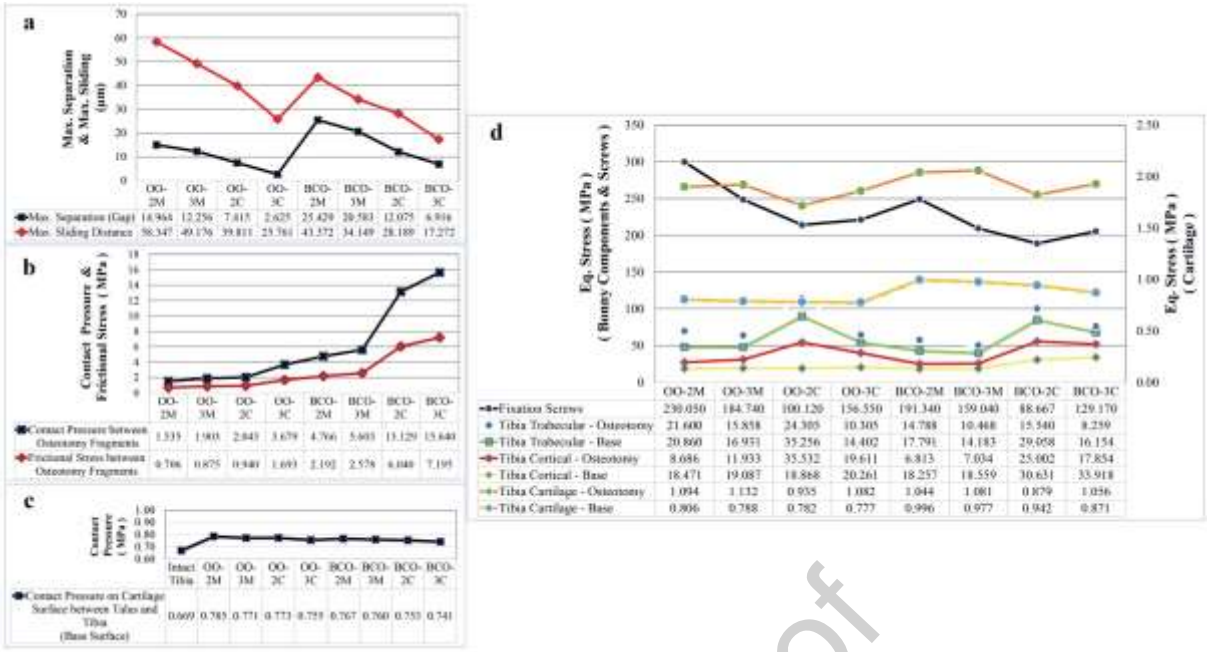

Figure 4. The summary of all results is presented in graphs. (a) Maximum sliding and separation. (b) Contact pressure and the frictional stress across the osteotomy plane. (c) Contact pressure on the tibiotalar articular surface. (d) Maximum equivalent stress by the components of the model.

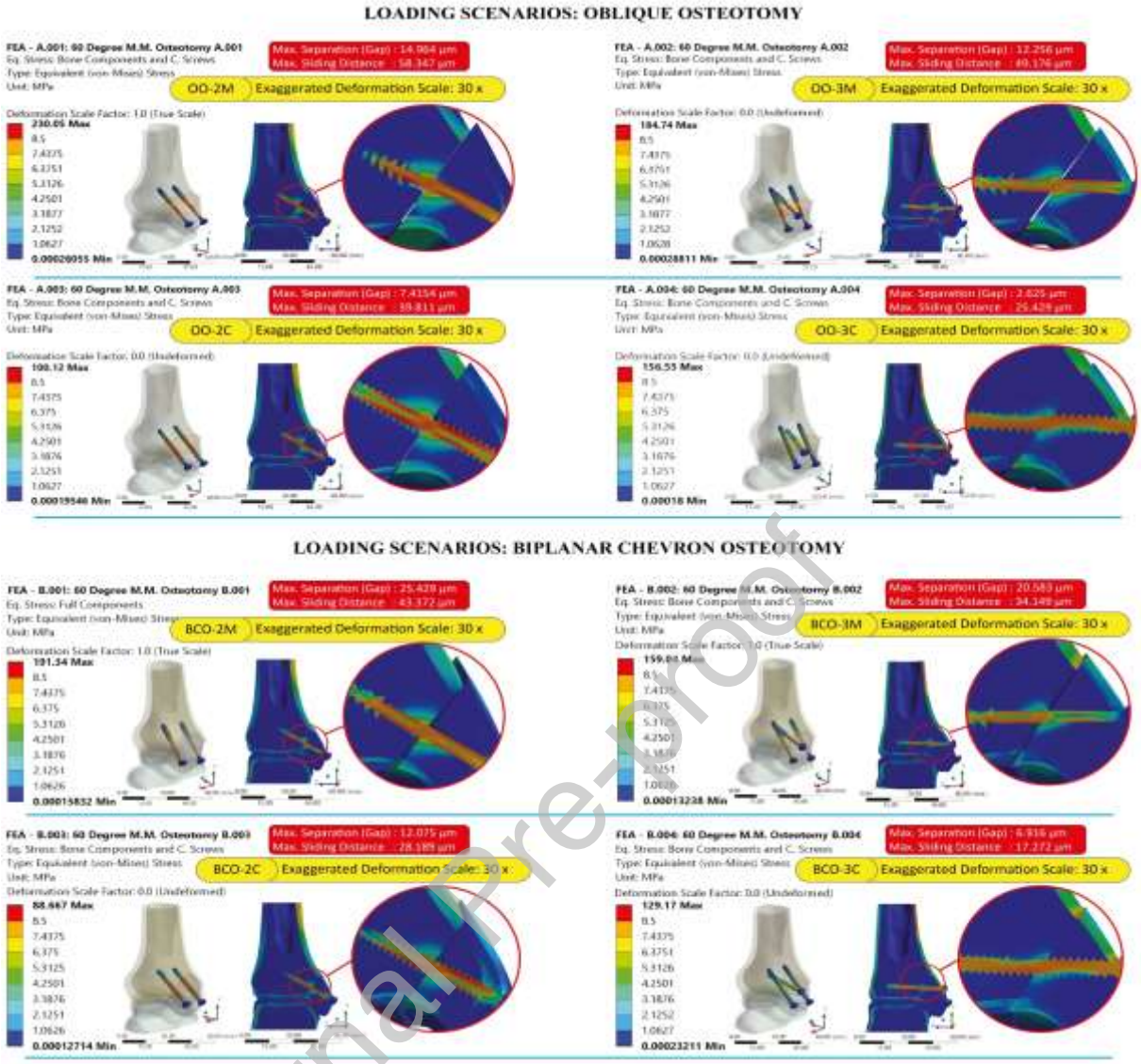

Figure 5. Visual outputs of the simulations showing von-Mises stress, sliding and separation of the osteotomy.

Table 1. Friction coefficients and fixation screw preload assigned in the FEA set up.

References are provided as uppercase numbers.

Parameters		**Value**
Coefficient of Friction between	Cartilage and Cartilage	0.0164[21]
	Bony Parts and Fixation Screw	0.37[22, 23]
	Bony Parts	0.46[24]
Fixation Screw Preload (N)		2.5[25]

Table 2. Material properties assigned in the FEA set up in accordance with the homogenous isotropic linear elastic material model. References are provided as uppercase numbers.

Parameters	**Unit**	**Model Components**			
		Cortical Bone	**Trabecular Bone**	**Cartilage**	**Fixation Screws (Ti-6Al-4V)**
Modulus of Elasticity	(MPa)	19100[26, 27]	1000.61[28, 29]	12[30, 31, 32]	115000[33]
Poisson's Ratio	(-)	0.3[30]	0.3[30]	0.42[31, 32]	0.33[33]
Density	(kg m^{-3})	1980[30]	830[34]	431[30]	4500[33]